*Progress In Electromagnetics Research B, Vol. 15, 347–373, 2009*

# LINEAR AND CIRCULAR ARRAY OPTIMIZATION: A STUDY USING PARTICLE SWARM INTELLIGENCE

**M. Khodier and M. Al-Aqeel**

Department of Electrical Engineering
Jordan University of Science & Technology
P. O. Box 3030, Irbid 22110, Jordan

**Abstract**—Linear and circular arrays are optimized using the particle swarm optimization (PSO) method. Also, arrays of isotropic and cylindrical dipole elements are considered. The parameters of isotropic arrays are elements excitation amplitude, excitation phase and locations, while for dipole array the optimized parameters are elements excitation amplitude, excitation phase, location, and length. PSO is a high-performance stochastic evolutionary algorithm used to solve $N$-dimensional problems. The method of PSO is used to determine a set of parameters of antenna elements that provide the goal radiation pattern. The effectiveness of PSO for the design of antenna arrays is shown by means of numerical results. Comparison with other methods is made whenever possible. The results reveal that design of antenna arrays using the PSO method provides considerable enhancements compared with the uniform array and the synthesis obtained from other optimization techniques.

## 1. INTRODUCTION

The methods used for the synthesis of antenna arrays can be broadly classified into two categories: deterministic and stochastic. The deterministic methods include analytical methods [1–8] and semi-analytical methods [9–15]. The deterministic methods in general become quite involved and computationally time consuming as the number of the elements in the array increases.

On the other hand, stochastic methods are now very common in electromagnetics, and have many advantages over deterministic

Corresponding author: M. Khodier (majidkh@just.edu.jo).

methods [16]. These methods include neural networks (NN) [17–19] and evolutionary algorithms such: genetic algorithm (GA) [20–32], simulated annealing (SA) [33–36], differential evolution (DE) [37], and Tabu search (TS) [38]. The advantages of using stochastic methods are their ability in dealing with large number of optimization parameters, avoiding getting stuck in local minima, and relatively easy to implement on computers. Another recently invented evolutionary, high-performance algorithm is the particle swarm optimization (PSO) method introduced in [39, 40]. It requires fewer lines of code than GA or SA and easier to implement. Another advantage of PSO against GA is the small number of parameters to be tuned. In PSO, the population size, the inertial weight and the acceleration constants summarize the parameters to be scaled and tuned, whereas in GA the population size, the selection, crossover and mutation strategies, as well as the crossover and mutation rates influence the result [41]. Also, [41] shows that PSO algorithm convergence is faster than GA and SA for the same problem and the main computational time is lower than SA, binary GA, real GA, binary hybrid GA, and real hybrid GA. The literature on the use of the PSO method in the design of antenna arrays is extensive, a sample of which can be found in [42–57]. In this paper, the method of PSO is used to provide a comprehensive study of the design of linear and circular antenna arrays. The parameters of antenna elements that provide the goal radiation pattern are optimized using the PSO. The effectiveness of PSO for the design of antenna arrays is shown by means of numerical results. Comparison with other methods is made whenever possible. The results reveal that design of antenna arrays using the PSO method provides considerable enhancements compared with the uniform array and the synthesis obtained from other optimization techniques.

## 2. LINEAR ANTENNA ARRAY

An $2N$-element array distributed symmetrically along $x$-axis is considered as shown in Figure 1. The array factor is

$$AF(\phi) = 2\sum_{n=1}^{N} I_n \cos[kx_n \cos(\phi) + \varphi_n] \tag{1}$$

where $k$ is the wavenumber, and $I_n$, $\varphi_n$ and $x_n$ are, respectively, the excitation amplitude, phase, and location of element $n$. The element number 1 ($n = 1$) is placed at $x_1 = \lambda/4$.

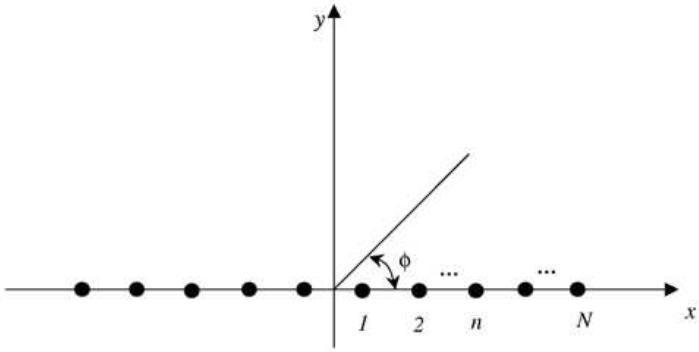


**Figure 1.** Geometry of the $2N$-element symmetric linear array placed along the $x$-axis.

### 2.1. Minimize the Maximum SL Peak

The PSO algorithm is used to obtain the optimum synthesis of a $2N$-element linear array in order to minimize the maximum SLL in a specific region. The fitness function is formulated as

$$\begin{aligned} \text{fitness} = & \min\left(\max\left\{20\log|AF(\phi)|\right\}\right) \\ & \text{subject to } \phi \in \{[0°, 76°]\&[104°, 180°]\} \end{aligned} \tag{2}$$

*2.1.1. Optimize Elements Amplitude $I_n$*

Here, we optimize $I_n$'s of the array and fix $\varphi_n$'s and $x_n$'s. The fixed parameters are those of the uniform array, i.e., $\varphi_n = 0$ and the spacing between elements is $\lambda/2$, $n = 1, \ldots, N$. The initial values of the amplitudes are set to be uniformly distributed from $[0, 1]$. The search region for each agent in the swarm is from $[0, 1]$. The normalized results from the optimization are given in Table 1. Also a Chebyshev array

**Table 1.** $2N = 10$ elements optimized using PSO with respect to amplitudes constraint compared with Chebyshev method with maximum SLL $= -24.6217$ dB (the values are normalized).

| **Element** | **1** | **2** | **3** | **4** | **5** |
|---|---|---|---|---|---|
| $\|I_n\|$ **PSO** | 1.0000 | 0.9010 | 0.7255 | 0.5120 | 0.4088 |
| $\|I_n\|$ **Cheby.** | 1.0000 | 0.9010 | 0.7255 | 0.5119 | 0.4088 |

that results in the same SLL is shown in the same table. The amplitude distributions along the array elements are shown in Figure 2(b). The values of the amplitude are decreasing from the center of the array to the edges. The corresponding radiation pattern in the azimuth plane ($x$-$y$ plane) compared with uniform array is shown in Figure 2(a). The maximum SLL obtained is $-24.6217$ dB while the maximum SLL of the uniform one is $-13$ dB. The proposed array SLL is less than the uniform one of about 11.6 dB. The smooth amplitude distribution makes it possible to use power dividers. However, from Figure 2(a) we note that the beamwidth of the optimized array is slightly larger than the conventional one since it is well known that the uniform array is optimum in terms of beamwidth. Nevertheless, the difference between the two is very small. Recently in [38], linear array's element

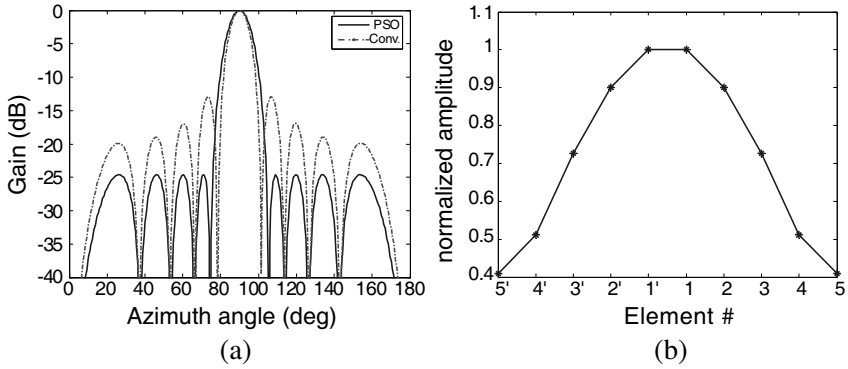


**Figure 2.** (a) Radiation pattern of 10 elements $\lambda/2$ spaced array optimized with PSO with respect to amplitudes, compared with conventional array. (b) Normalized amplitude distribution $\|I_n\|$ of array elements using PSO in Table 1.

**Table 2.** $2N = 16$ elements optimized using PSO with respect to amplitudes using (3) and (4) constraint compared with TSO and Chebyshev methods with maximum SLL $= -30.7$ dB (the values are normalized).

| Element | 1 | 2 | 3 | 4 | 5 | 6 | 7 | 8 | SLL [dB] |
|---|---|---|---|---|---|---|---|---|---|
| $\|I_n\|$ **TS [38]** | 1.0000 | 0.9627 | 0.8766 | 0.7560 | 0.6105 | 0.4833 | 0.2957 | 0.3426 | −30.4 |
| $\|I_n\|$ **PSO** | 1.0000 | 0.9521 | 0.8605 | 0.7372 | 0.5940 | 0.4465 | 0.3079 | 0.2724 | −30.7 |
| $\|I_n\|$ **Cheby.** | 1.0000 | 0.9515 | 0.8602 | 0.7364 | 0.5933 | 0.4457 | 0.3069 | 0.2713 | −30.7 |

amplitudes are optimized using the Tabu search optimization method (TSO) to minimize the maximum SLL. The results obtained from PSO versus TSO result are tabulated in Tables 2 and 3 for 16-element array and 24-element array, respectively. Also, values of Chebyshev array are given in the tables where the maximum SLL is the same from PSO method.

From Tables 1–3, we see that the PSO results are almost identical to Chebyshev one. Also, the maximum SLL obtained from PSO is less than the TSO method in all cases. In [38], a comparison is made between TSO and Chebyshev algorithm and the results are not identical. Figures 3 and 4 illustrate the array factor compared with conventional array, and the amplitude distribution of PSO compared with TSO in Tables 2 and 3.

**Table 3.** $2N = 24$ elements optimized using PSO with respect to amplitudes constraint compared with TSO and Chebyshev methods with maximum SLL $= -34.5$ dB (the values are normalized).

| **Optimization method** | | **SLL [dB]** |
|---|---|---|
| $\|I_n\|$ **TS [38]** | 1.0000,0.9811,0.9373,0.8850,0.7883,0.7294, 0.5984,0.5319,0.4051,0.3381,0.2123,0.3197 | $-33.0$ |
| $\|I_n\|$ **PSO** | 1.0000,0.9712,0.9226,0.8591,0.7812,0.6807, 0.5751,0.4768,0.3793,0.2878,0.2020,0.2167 | $-34.5$ |
| $\|I_n\|$ **Cheby.** | 1.0000,0.9758,0.9289,0.8619,0.7787,0.6839, 0.5824,0.4794,0.3795,0.2870,0.2049,0.2225 | $-34.5$ |

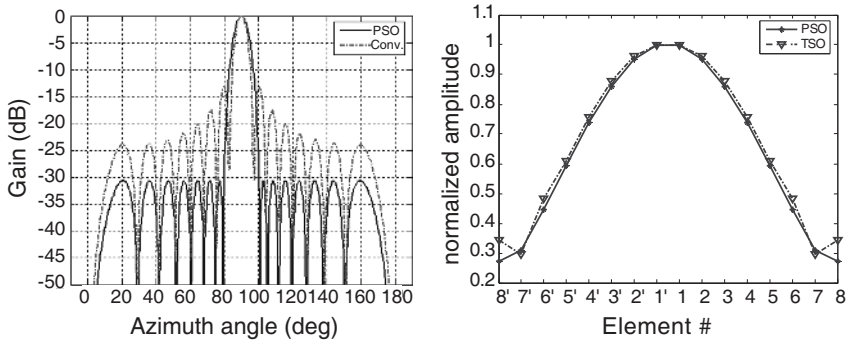


**Figure 3.** (a) Radiation pattern of 16 elements $\lambda/2$ spaced optimized using PSO with respect to amplitudes, compared with conventional array. (b) Normalized amplitude distribution.

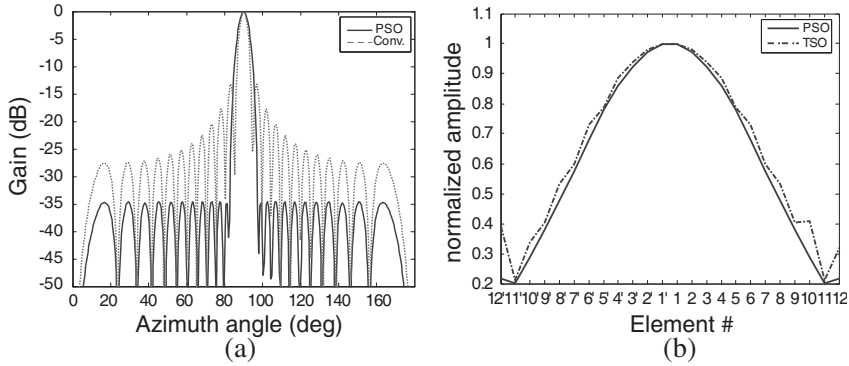


**Figure 4.** (a) Radiation pattern of 24 elements $\lambda/2$ spaced optimized using PSO with respect to amplitudes, compared with conventional array. (b) Normalized amplitude distribution.

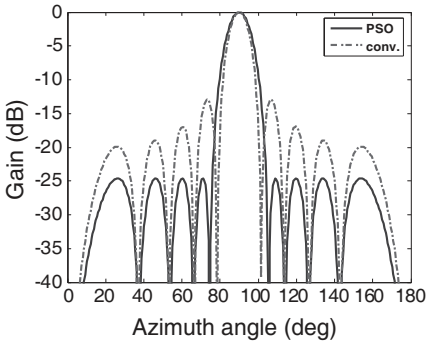


**Figure 5.** Radiation pattern of 10 elements $\lambda/2$ spaced, optimized with respect to phases compared with the uniform phases conventional case.

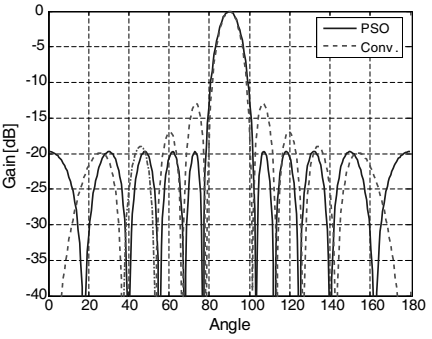


**Figure 6.** Radiation pattern of 10-elements linear array positions optimized using (3) compared with the uniform case.

### *2.1.2. Optimize Elements Phases $\varphi_n$*

We fixed $I_n = 1$ and the spaces between elements is $\lambda/2$ as the uniform array. The first element phase is fixed to $\varphi_1 = 0°$. Initial phase values are uniformly distributed in $[0, 180°]$. Table 4 shows the corresponding phases of the array.

Figure 5 shows the radiation pattern of the array compared with uniform array and the maximum SLL is $-24.62$ dB which is higher than the case were the amplitudes are non-uniform of only 0.0017 dB, but still better than the uniform one in terms of SLL.

**Table 4.** $2N = 10$ elements optimized with respect to phases.

| **Element** | **1** | **2** | **3** | **4** | **5** |
|---|---|---|---|---|---|
| $\varphi_n$ **[deg]** | 00.0000 | 25.7120 | 43.4847 | 59.2084 | 64.8670 |

**Table 5.** $2N = 10$ elements optimized with respect to positions.

| **Element** | **1** | **2** | **3** | **4** | **5** |
|---|---|---|---|---|---|
| $\pm x_n[\lambda]$ | 0.2146 | 0.5999 | 1.0611 | 1.5870 | 2.2500 |

The smooth phase distribution may allow using delay circuit to perform the needed phase shifts.

*2.1.3. Optimize Element Positions $x_n$*

We fix the amplitudes and phases as the case of $\lambda/2$ spaced conventional array ($I_n = 1$ and $\varphi_n = 0°$), and adjust the positions $x_n$'s by the PSO. The total length of a 10-elements, $\lambda/2$ spaced uniform array is $4.5\lambda$. Therefore, we fix the last elements positions to $x_{\pm N} = \pm 2.25\lambda$, and the problem is solved in a four-dimensional solution space. The minimum distance between two neighboring elements is $|x_i - x_j| = 0.25\lambda$, where $i = 1, 2, 3, 4$ and $i \neq j$. This leads to $\min(x_i) = 0.125\lambda$.

The optimum element positions obtained from PSO are given in Table 5. The relative radiation pattern is shown in Figure 6 along with the $\lambda/2$ spaced conventional array pattern. It should be mentioned here that our results exactly matches the results in [45]. The maximum peak in the SLL region is about $-19.7167$ dB which is lower of about 6.7 dB from the uniform array.

Some applications are interested in the minimizing the close-in SLL (the first sidelobe nearest to the main beam). To achieve this property, a modified fitness is used:

$$\begin{aligned} &\text{fitness} = \min(\alpha_1 \max\{20\log|AF(\phi_{AS})|\} \\ &+\alpha_2 \max\{20\log|AF(\phi_{NS})|\}) \qquad (3) \\ &\text{subject to } \phi_{AS} \in \{[0°, 76°]\&[104°, 180°]\} \\ &\text{and } \ \phi_{NS} \in \{[69°, 76°]\&[104°, 111°]\} \qquad (4) \end{aligned}$$

This fitness function has an advantage of controlling the near sidelobe. The region specified by $\phi_{AS}$ is the same region as (2) and $\alpha_1$ is its weight. The close-in sidelobe region is specified by $\phi_{NS}$ and $\alpha_2$. This modification allows the near sidelobe region to be controlled and the amount of its reduction depends on the values of $\alpha_1$ and $\alpha_2$.

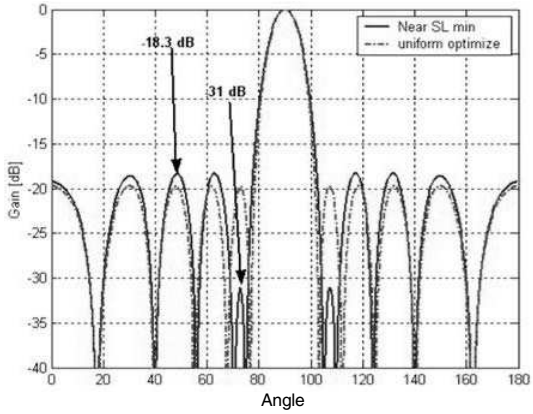


**Figure 7.** Radiation pattern of 10 elements array positions optimized in Table 6 compared with the array in Table 5.

**Table 6.** $2N = 10$ elements optimized with respect to positions.

| **Element** | **1** | **2** | **3** | **4** | **5** |
|---|---|---|---|---|---|
| $\pm x_n[\lambda]$ | 0.1685 | 0.5461 | 0.9364 | 1.5107 | 2.25 |

For example, a 10-element linear array is optimized using the fitness function given by (3) and weights $\alpha_1 = 1$ and $\alpha_2 = 2$. Table 6 shows the array elements positions and Figure 7 shows the difference between radiation pattern of the modified array and the array in Table 5.

Although the far sidelobe region is about $-18.3$ dB which is higher than the previous case of about 1.4 dB, the near sidelobe is minimized to $-31$ dB and the reduction is about 11.3 dB from the previous case and about 18 dB from $\lambda/2$ spaced uniform array.

*2.1.4. Optimize Array Amplitudes ($I_n$), Phases ($\varphi_n$) and Separations ($x_n$)*

Here, all array parameters are optimized. The first element phase is set to zero as a reference to other elements. The initial elements positions are set as in the $\lambda/2$ spaced uniform array, and the edge elements are set to $\pm(N - 0.5)(\lambda/2)$ which is also used as the upper limit for the positions. The lower limit is defined as $\pm 0.25(\lambda/2)$. So the positions searching region can be defined as $0.25\lambda/2 < x_n < (N - 1/2)(\lambda/2)$ where $n = 1, \ldots, (N - 1)$.

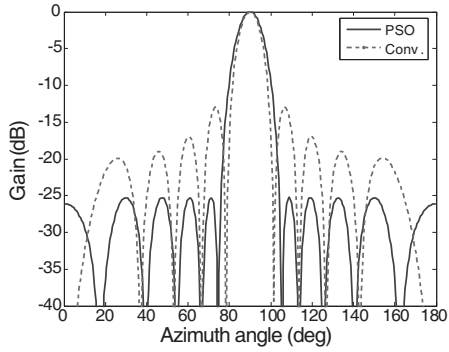


**Figure 8.** Radiation pattern of 10-elements array positions optimized with respect to amplitudes ($I_n$), phases ($\phi_n$) and separations ($x_n$) compared with $\lambda/2$ spaced uniform array.

**Table 7.** $2N = 10$ elements optimized with respect amplitudes ($I_n$), phases ($\varphi_n$) and separations ($x_n$) using (2).

| **Element** | **1** | **2** | **3** | **4** | **5** |
|---|---|---|---|---|---|
| $\varphi_n$ **[deg]** | 0 | 40.49 | 54.24 | 49.46 | 51.97 |
| $\|I_n\|$ | 1.0000 | 0.82 | 0.94 | 0.96 | 0.72 |
| $x_n[\lambda]$ | 0.28 | 0.77 | 1.10 | 1.61 | 2.25 |

The PSO produced an array with parameters given in Table 7. The corresponding radiation pattern is shown in Figure 8 compared with $\lambda/2$ spaced conventional array. The maximum SLL here is $-25.271$ dB which is 12.271 dB lower than the $\lambda/2$ spaced conventional array, 0.644 dB lower than the arrays in Sections 2.1.1 and 2.1.2 and 5.555 dB lower than the array in Section 2.1.3. The array parameters obtained are different than the parameters obtained in the previous three sections. Also, we can see from Table 7 that the current and phase distributions are not smooth like the results in Sections 2.1.1 and 2.1.2. The enhancement here is good compared to the conventional and Section 2.1.3 arrays, but it is not much different from Sections 2.1.1 and 2.1.2 arrays.

## 2.2. Minimize the SL Average Power

In this section, we are interested in the design of linear antenna array with minimum average SL power. To achieve this goal, the following

function is used to evaluate the fitness:

$$\text{fitness} = \min\left(\sum_i \frac{1}{\Delta\phi_i}\int_{\phi_{li}}^{\phi_{ui}} |AF(\phi)|^2\, d\phi\right) \tag{5}$$

where $[\phi_{li}, \phi_{ui}]$ is the spatial regions in which the SLL is suppressed and $\Delta\phi_i = \phi_{ui} - \phi_{li}$. The sidelobe regions are specified by

$$\phi_{l1} = 0^\circ, \quad \phi_{u1} = 81^\circ, \quad \phi_{l2} = 99^\circ, \quad \phi_{u2} = 180^\circ. \tag{6}$$

The integration in (5) doesn't have a closed form and should be evaluated numerically. For this purpose, we use a 32 point Gaussian-Legender method.

### *2.2.1. Optimize Element Amplitudes $I_n$*

The amplitudes are initialized randomly within the interval [0, 1] which also represents the searching region. Table 8 shows the corresponding amplitudes and Figure 11 shows the array radiation pattern compared with the pattern of conventional case.

It can be seen from Figure 9 that the conventional array exhibits relatively high SLL, while the PSO algorithm offers an improvement in terms of SLL suppression. Table 8 shows that the element amplitudes are decreasing from the center of the array to the edges.

**Table 8.** $2N = 10$ elements optimized with respect to amplitudes using (5).

| Element | 1 | 2 | 3 | 4 | 5 |
|---|---|---|---|---|---|
| $\|I_n\|$ | 1.000 | 0.8122 | 0.6799 | 0.5655 | 0.3546 |

### *2.2.2. Optimize Element Phases $\varphi_n$*

Element amplitudes $I_n$'s and positions $x_n$'s are fixed as the $\lambda/2$ spaced conventional array. As a reference, the first element phase is fixed to zero. The result found by the PSO algorithm is the same as the conventional array, i.e., $\varphi_n = 0^\circ$ for all $n = 1, 2, \ldots, N$, and we can say that the $\lambda/2$ spaced conventional array is optimum in the sense of minimizing (5).

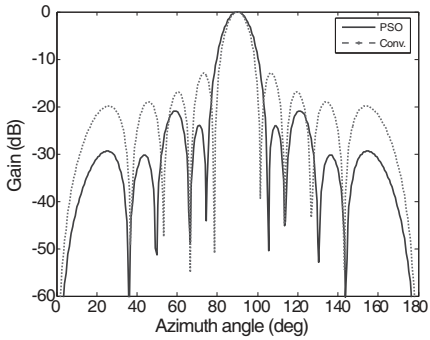


**Figure 9.** Radiation pattern of 10 elements positions optimized with respect to amplitudes ($I_n$), and compared with conventional array.

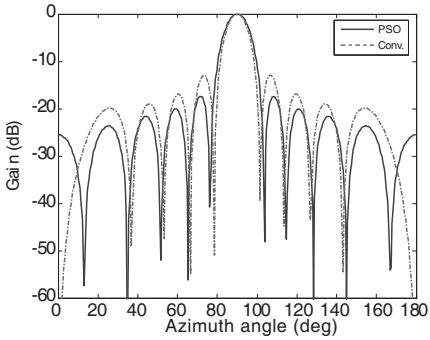


**Figure 10.** Radiation pattern of 10-element array optimized with respect to positions $x_n$'s, compared with conventional array.

**Table 9.** $2N = 10$ array optimized with respect to element positions using (5).

| Element | 1 | 2 | 3 | 4 | 5 |
|---|---|---|---|---|---|
| $d_n[\lambda]$ | 0.2529 | 0.5558 | 1.0635 | 1.4990 | 2.1101 |

### *2.2.3. Optimize Element Positions $x_n$*

Here, we freed the total array length and did not fix it as in previous sections. Initial positions for the PSO are as the $\lambda/2$ spaced conventional array to speed the PSO convergence. The searching region is within the interval $[0.125,\ (N/2) - 0.5]\ \lambda/2$. The array geometry obtained from PSO is shown in Table 9 which exactly matches the result in [42]. It can be seen from the table that the array length obtained using the PSO algorithm is less than the conventional array. The radiation pattern in Figure 10 shows more enhancements compared to the conventional array.

### *2.2.4. Optimize Element Amplitudes $I_n$, Phases $\varphi_n$ and Separations $x_n$*

Table 10 shows the PSO results for amplitudes $I_n$'s, phases $\varphi_n$'s and separations $x_n$'s. The array aperture is larger than the conventional array and the array in Section 2.1.4. Amplitude distribution is not smooth as the array in Section 2.1.1. The phases of the array are

**Table 10.** $2N = 10$ array optimized with respect to element amplitudes $I_n$'s, phases $\varphi_n$'s and separations $x_n$'s.

| **Element** | 1 | 2 | 3 | 4 | 5 |
|---|---|---|---|---|---|
| $\varphi_n$ **[deg]** | 0.000 | 0.000 | 0.000 | 0.000 | 0.000 |
| $\|I_n\|$ | 1.000 | 0.5507 | 0.2761 | 0.5933 | 0.2913 |
| $x_n[\lambda/2]$ | 0.7356 | 2.2084 | 2.2151 | 3.6712 | 5.0000 |

exactly like the phases of the array in Section 2.2.2, which is the same as $\lambda/2$ spaced conventional array. So by controlling only elements amplitude and position, we can achieve an array with more SLL average reduction. The corresponding radiation pattern compared with the conventional one is plotted in Figure 11. The enhancement in the SSL average is more than the arrays obtained in Sections 2.2.1, 2.2.2 and 2.2.3.

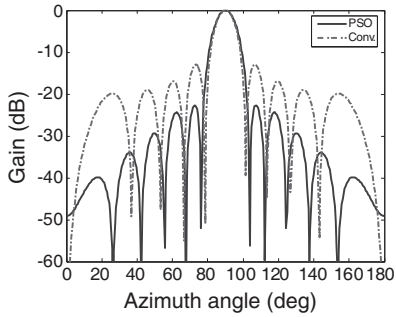


**Figure 11.** Radiation pattern of 10 elements optimized with respect to amplitudes ($I_n$), phases ($\varphi_n$) and separations ($x_n$) compared with $\lambda/2$ spaced uniform array.

## 2.3. Linear Array Beam Steering

This section illustrates the ability of PSO algorithm to perform linear array beam steering. Here, the SLL band is the regions beside the main beam in which its maximum occurred at the goal steering angle. Elements amplitude and position are fixed as those of the conventional array and only phases are optimized. The used array factor is

$$AF(\phi) = \sum_{n=2}^{2N} \exp\left(j[n\pi\cos(\phi) + \varphi_n]\right) + 1 \tag{7}$$

In (7), we assume uniform amplitude and positions, while setting $\varphi_1 = 0^\circ$ as a reference. The sidelobe region is defined as

$$\phi_{SLL} \in \left\{ \left[0^\circ, \left(\phi_d - \frac{\Delta\phi_d}{2}\right)^\circ\right], \left[\left(\phi_d + \frac{\Delta\phi_d}{2}\right)^\circ, 180^\circ\right] \right\} \quad (8)$$

where $\phi_d$ is the steering angle, and $\Delta\phi_d$ is the band where $\phi_d$ is included. The result for 20-element array are shown in Table 11. The array factor is plotted in Figure 12(a) with $\lambda/2$ spaced conventional array steered towards the same angle pattern as in [5], respectively. Element phases are plotted in Figure 12(b). Another example for a 20-element array with $\phi_d = 45^\circ$ and $\Delta\phi_d = 22^\circ$ optimized to minimize the maximum SLL is shown in Figure 13. The SLL reduction in this case is considered only in the near SL region but the array SLL obtained is larger than the conventional array in far SL region.

**Table 11.** 20-elements array optimized with respect to phases to radiate towards $\phi_d = 45^\circ$ with $\Delta\phi_d = 14^\circ$.

| | |
|---|---|
| $\varphi_n$[deg] Uniform array | 000.0,232.7,105.4,338.2,210.9,083.6,316.3, 189.0,061.8,294.5,167.2,039.9,272.6,145.4, 018.1,250.8,123.5,356.3,229.0,101.7. |
| $\varphi_n$[deg] PSO array | 0.000,253.0,134.0,006.5,237.9,109.7,343.3, 217.1,091.3,324.8,197.8,070.9,304.9,179.0, 051.8,284.6,156.1,028.8,268.8,165.9. |

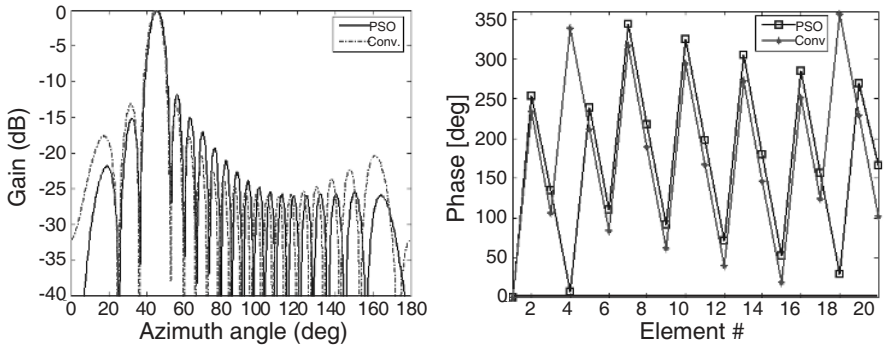


**Figure 12.** (a) Radiation pattern of 20-elements linear array optimized with respect to phases $\varphi_n$'s to radiate towards $\phi_d = 45^\circ$ with $\Delta\phi_d = 14^\circ$. (b) The corresponding element phases compared with $\lambda/2$ spaced conventional array steered towards $\phi_d = 45^\circ$.

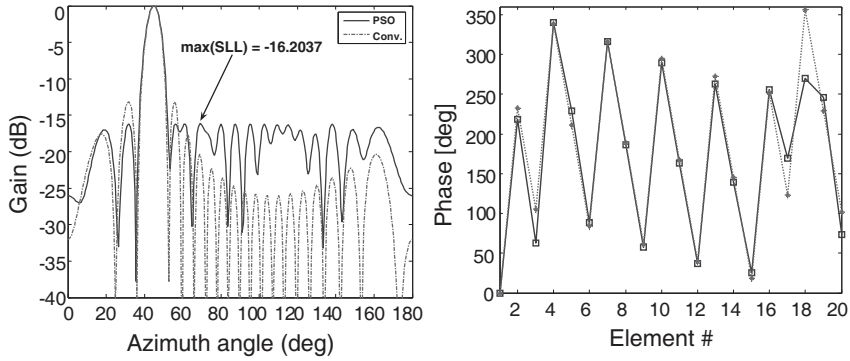


(a) (b)

**Figure 13.** (a) Radiation pattern of 20-elements linear array optimized with respect to phases $\varphi_n$'s to minimize the maximum SLL and radiate towards $\phi_d = 45°$ with $\Delta\phi_d = 22°$. (b) The corresponding element phases compared with $\lambda/2$ spaced conventional array steered towards $\phi_d = 45°$.

## 3. CIRCULAR ARRAY OPTIMIZATION

The PSO method is also employed to determine an optimum set of weights and/or antenna element separations to create a non-uniform circular isotropic array that maintains low side lobes. Also, dipole circular arrays are widely used in communication systems as the components for signal receiving [58]. Therefore, circular dipole array are also considered here to determine the optimum set of excitations, antenna elements separations and dipoles lengths.

### 3.1. Isotropic Circular Array

We consider isotropic circular array and optimize the radiation pattern of the array in the term of the SLL reduction. The PSO algorithm is used to determine the complex weights $\alpha_n$ and/or the separation between elements $dm_n$ where $n = 1, \ldots, N$ and $N$ is the total number of elements in the array. The array geometry is shown in Figure 14 for an array of $N$ elements. The array factor for such array is given in [59] as:

$$AF(\phi, \alpha, dm) = \sum_{n=1}^{N} \alpha_n e^{j(ka\cos(\phi-\phi_n))} \tag{9}$$

$$\alpha_n = I_n e^{j\varphi_n} \tag{10}$$

$$ka = \sum_{i=1}^{N} dm_i \tag{11}$$

$$\phi_n = 2\pi \sum_{i=1}^{n} dm_i \Big/ \sum_{i=1}^{N} dm_i \tag{12}$$

$I_n, \varphi_n$ represents the amplitude and the phase excitation of the $n$th element in the array with respect, $dm_n$ represents the separation (arc longitude) from element $n$ to element $n+1$, $k = 2\pi/\lambda$ the wave number, $\phi$ is the angle of incidence of a plane wave and $\lambda$ is the signal wavelength. From the previous array factor we can formulate the objective function for the PSO to be optimized. Let $AF(\alpha, \phi_{msl}, dm)$ is the value of the array factor where the maximum sidelobe is attained at $\phi_{msl}$ within the scanning ranges $[0, \phi_1]$ and $[\phi_2, 360]$. The array will direct its main beam towards the angle $\phi_{dis}$, and the fitness function is formulated as

$$\text{fitness} = \min(\max(20 * \log(AF(\alpha, \phi_{msl}, dm)/AF(\alpha, \phi_{dis}, dm))) \quad \text{Subject to } dm_n \leq D \tag{13}$$

where $D$ is the maximum arc separation between element $n$ and element $n+1$. The PSO algorithm is applied to optimize circular isotropic array of ten elements while the scanning range is set to

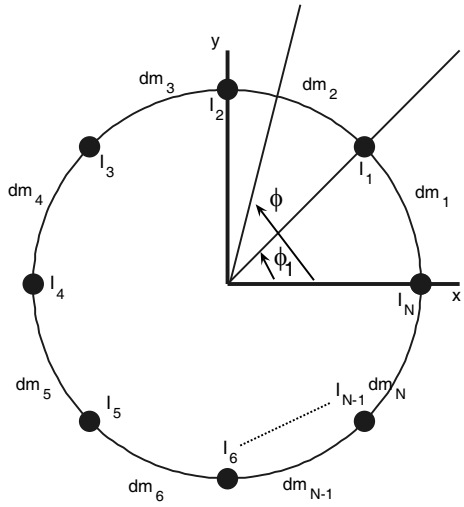


**Figure 14.** Isotropic circular array geometry.

$[0, 158]°$and $[202, 360]°$. Table 12 shows the result obtained from PSO where $D = 2\lambda$ and the result obtained from genetic algorithm (GA) in [59]. From Table 12 we see that the PSO maximum sidelobe is less than GA result of about 1.5 dB and 0.262 dB of [60] where the PSO with multi-objective fitness function is used to minimize the first null beamwidth (FNBW), the average SL power and the maximum SLL. The beamwidth is also narrower of about 1.44° compared to [59] and about 0.23° compared to [60]. The aperture reduction is about $0.07\lambda$ from [59] but it is larger than [60] of about $0.108\lambda$. Figure 15(a) shows

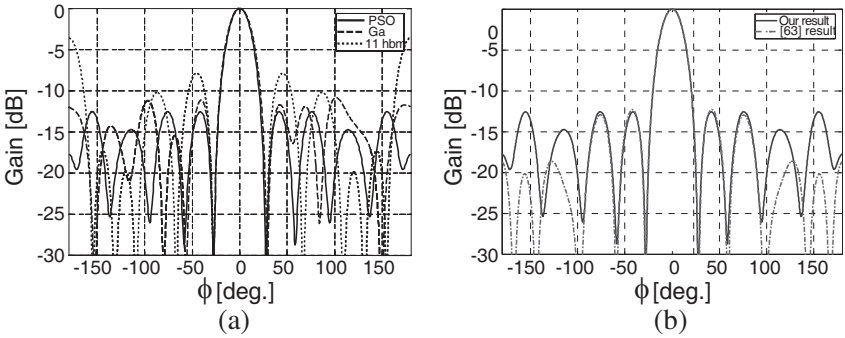


**Figure 15.** (a) Radiation pattern for circular isotropic array of 10 elements optimized with respect to $I$, $d_m$ as in Table 12 compared with the result from GA in [59] and the uniform array for $D = 2\lambda$. (b) PSO result in (a) compared with [60] result.

**Table 12.** $N = 10$ elements isotropic circular array optimized with respect to excitations amplitude and phase and elements separation in the range $[0, 158]°$ and $[202, 360]°$.

| | | | |
|---|---|---|---|
| **Uniform array** | $I_n$ | **1, 1, 1, 1, 1, 1, 1, 1, 1, 1** | **Max(SLL) = –3.6 dB** |
| | $dm_n/\lambda$ | **0.5, 0.5, 0.5, 0.5, 0.5, 0.5, 0.5, 0.5, 0.5, 0.5** | **Aperture = 5 λ** **3 dB BW = 25.8 deg** |
| **GA [59]** | $I_n$ | **0.9545, 0.4283, 0.3392, 0.9074, 0.8086, 0.4533, 0.5634, 0.6015, 0.7045, 0.5948** | **Max(SLL) = –11.03 dB** |
| | $dm_n/\lambda$ | **0.3641, 0.4512, 0.2750, 1.6373, 0.6902, 0.9415, 0.4657, 0.2898 ,0.6456, 0.3282** | **Aperture = 6.08 λ** **3 dB BW = 25.46 deg** |
| **PSO [60]** | $I_n$ | **1.0000, 0.7529, 0.7519, 1.0000, 0.5062, 1.0000, 0.7501, 0.7524, 1.0000, 0.5067** | **Max(SLL) = –12.307 dB** |
| | $dm_n/\lambda$ | **0.3170, 0.9654, 0.3859, 0.9654, 0.3185, 0.3164, 0.9657, 0.3862, 0.9650, 0.3174** | **Aperture = 5.9029 λ** **3 dB BW = 24.34 deg** |
| **PSO (our work)** | $I_n$ | **0.7383, 0.8737, 0.5782, 1.000 0.7088, 1.000, 0.5782, 0.8737 0.7383, 0.7179** | **Max(SLL) = –12.5687 dB** |
| | $dm_n/\lambda$ | **0.3243, 0.9747, 0.4124, 0.9369, 0.3571 0.3572, 0.9369, 0.4124, 0.9747, 0.3243** | **Aperture = 6.0109 λ** **3 dB BW = 24.02 deg** |

the PSO obtained radiation pattern, compared with GA result [59] and the uniform array. Figure 15(b) shows the obtained radiation pattern compared with the PSO result in [60]. It is clearly seen that the far SLL is larger than that in [60].

More enhancements can be obtained if the excitations phase $\varphi_n$ is also optimized. The result is shown in Table 13 for the same case in Table 12. From Table 13, the enhancement appears clearly in SLL, aperture and 3 dB beamwidth. From Figure 16 we can see the difference between the two cases. Also, the obtained array has better

**Table 13.** $N = 10$ elements isotropic circular array optimized with respect to excitations amplitude and phase and elements separation in the range $[0, 158]^\circ$ and $[202, 260]^\circ$.

| | | |
|---|---|---|
| $I_n$ | **0.2478 0.9149 0.8054 0.5610 1.0000 0.5610 0.8054 0.9149 0.2478 0.8254** | **Max(SLL)=−15.2853 dB Aperture=5.7929$\lambda$ 3 dB BW=22.54deg** |
| $dm_n/\lambda$ | **0.5462 0.6220 0.7513 0.4910 0.4859 0.4860 0.4910 0.7513 0.6220 0.5462** | |
| $\varphi_n$ | **−33.3758, 11.5900, 48.9874, 32.5824, 0, 32.5824, 48.9874, 11.5900, −33.3758, 48.5313** | |

**Table 14.** $N = 10$ elements isotropic circular array optimized with respect to excitations amplitude and phase and to elements separation in the range $[0, 158]^\circ$ and $[202, 360]^\circ$ for $D = \lambda/2$.

| | | |
|---|---|---|
| $I_n$ | **1.0000 0.9539 0.6929 0.8307 0.5462 0.8307 0.6929 0.9539 1.0000 0.6702** | **Max(SLL)=−11.8441 dB Aperture=4.5303$\lambda$ 3 dB BW=24.98deg** |
| $d_n/\lambda$ | **0.4986 0.4613 0.3180 0.4906 0.4993 0.4940 0.4906 0.3180 0.4613 0.4986** | |
| $\varphi_n$ | **0 36.2445 60.0777 78.1235 −20.5532 78.1235 60.0777 36.2445 0 94.2095** | |

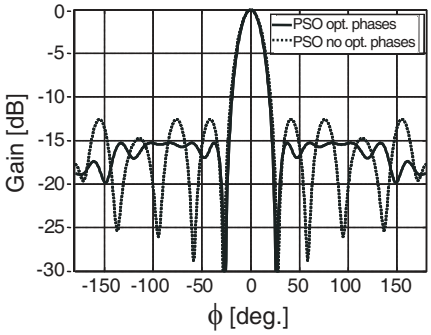


**Figure 16.** Radiation pattern for circular isotropic array of 10 elements optimized with respect to $I, \varphi, d_m$ as in Table 13 compared with the result of optimize $I, d_m$ for $D = 2\lambda$.

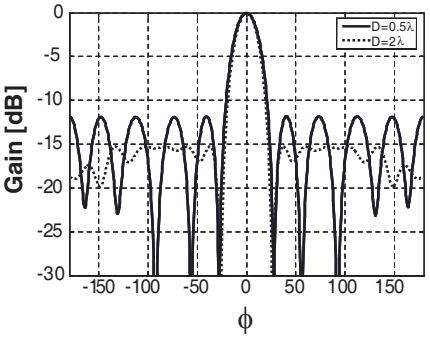


**Figure 17.** Radiation pattern for circular isotropic array of 10 elements optimized with respect to $I, \varphi, d_m$ for $D = \lambda/2$ as in Table 14 compared with the result of optimize $I, \varphi, d_m$ for $D = 2\lambda$.

properties than one in [60].

From the above examples, we see that more enhancements could be achieved every time we include more array parameters in the PSO algorithm, but all the time we get a result for the array aperture more than the uniform one. To deal with this situation, we can limit the maximum separation $D$. Table 14 shows the results obtained when the separation is set to $D = \lambda/2$, where the aperture obtained is $4.53\lambda$ and the maximum SLL is $-11.84$ dB. The same thing can be said about the beamwidth which is 24.98° compared with 25.8° degree for the uniform case. Figure 17 shows the radiation pattern compared with the case when the separation limit is $D = 2\lambda$. The obtained radiation pattern has equal ripples in the sidelobe region.

### 3.2. Circular Dipole Array Optimization

In this section, we deal with the more practical case that the elements of the circular array are dipoles. In optimizing circular dipole array, the parameters to be controlled are elements excitation (amplitude and phase), elements separation, elements radii and elements lengths. The radiation pattern from the array is shaped by these parameters. Figure 18 shows the proposed circular dipole array geometry. Analysis of circular dipole array is the same as isotropic circular array but here the elements are dipoles. Mutual coupling between elements affects the array properties and there is no closed form of the array pattern.

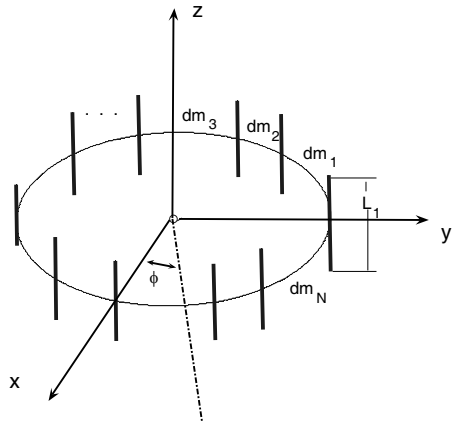


**Figure 18.** Circular dipole array geometry.

Numerical and approximate techniques are effectively used to obtain the array structure. The method of moments (MOM) is used to obtain the current distribution on the dipoles including mutual coupling effects. A common approximation is made by assuming that the current distribution along the dipole is sinusoidal (the current vanishes at the dipole terminals). This assumption becomes less accurate when the dipoles lengths are not a fraction of $\lambda/2$. So, we cannot use this assumption when the element lengths are optimized. We have to take into account that the elements lengths should be $\lambda/2$ if we want to use this assumption [61]. For a $z$-directed thin cylindrical antenna of length $l$ and radius $a$, with a current distribution $I(z)$ along its length, the Hallen's integral equation is given by [61]

$$\frac{\mu}{4\pi}\int_{-l/2}^{l/2} I(z')G(z-z')dz' = -j\omega\mu\varepsilon E_{in}(z) \tag{14}$$

where, $\mu$ the permeability of the material, $\varepsilon$ the permittivity of the material, $E_{in}$ the incident field, $\omega = 2\pi f$ and $f$ the frequency, $G(z-z') = \frac{e^{-jkR}}{R}$, $R = \sqrt{(z-z')^2 + a^2}$, and $a$ is the dipole radius.

The current $I(z)$ vanishes at the antenna ends, that is, $I(l/2) = I(-l/2) = 0$. If we assume that the dipole is fed from a gap in its center then the incident field value is determined from the fed voltage; it is zero for parasitic elements and none zero for active elements. The dipole is sampled into elements along the $z$-axis. Then, by solving the integral equation in (14) a system of equations is obtained from which that current distribution can be determined. From the current

distribution on the dipoles, the radiation pattern and the gain can be calculated.

We use the PSO algorithm to optimize the dipole circular array with respect to some of its parameters. First we fix the dipoles

**Table 15.** $N = 10$ elements dipole circular array optimized with respect to excitations amplitude and phase, and elements separation in the range $[0, 158]^\circ$ and $[202, 260]^\circ$ for $D = 2\lambda$.

| | | |
|---|---|---|
| $L_n/\lambda$ | **0.5000 0.5000 0.5000 0.5000 0.5000 0.5000 0.5000 0.5000 0.5000 0.5000** | **Max(SLL)=−17.3232 dB Aperture=5.4724$\lambda$ 3 dB BW=21.24deg** |
| $I_n$ | **1.0000 0.4265 0.7866 0.4141 0.3571 0.4141 0.7866 0.9066 1.0000 0.4265** | |
| $\varphi_n$ | **5.5947 45.7218 20.2796 −9.7969 −22.4059 −9.7969 −38.8068 45.7218 5.5947 20.2796** | |
| $dm_n/\lambda$ | **0.5275 0.5265 0.6203 0.5989 0.4630 0.4630 0.5989 0.6203 0.5275 0.5265** | |

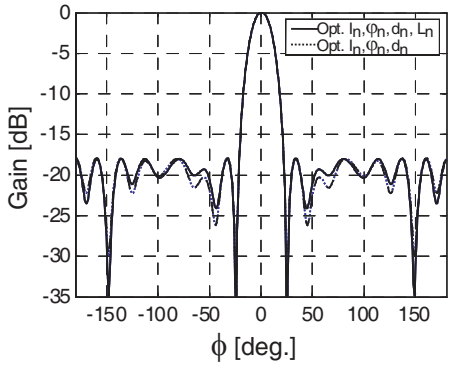


**Figure 19.** Radiation pattern for circular dipole array of 10 elements optimized with respect to $L, I, \varphi, d_m$ as in Table 16 compared with the result of optimizing $I, \varphi, d_m$ as in Table 15.

**Table 16.** $N = 10$ elements dipole circular array optimized with respect to excitations amplitude and phase, elements separation and elements lengths in the range $[0, 158]^\circ$ and $[202, 260]^\circ$ for $D = 2\lambda$.

| | | |
|---|---|---|
| $L_n$ | **0.5369 0.6094 0.5045 0.3232 0.5352 0.3232 0.5045 0.5364 0.5369 0.6094** | **Max(SLL)=−17.8819 dB Aperture=5.4751$\lambda$ 3 dB BW=21.18deg** |
| $I_n$ | **0.7481 1.0000 0.7312 0.5773 0.4411 0.5773 0.7312 1.0000 0.6957 0.7481** | |
| $\varphi_n$ | **−1.8166 −77.7446 55.3737 −33.6932 −41.1082 −33.6932 55.3737 −77.7446 −8.7745 −1.8166** | |
| $dm_n/\lambda$ | **0.4427 0.8849 0.1870 0.8297 0.6344 0.6344 0.8297 0.4427 0.8849 0.1870** | |

lengths and diameters and let the PSO algorithm determine the best excitations and separations in order to minimize the following fitness function

$$\text{fitness} = \min(\max(20 * \log(g(\phi_{msl}, \alpha, dm)/g(\phi_{dis}, \alpha, dm))) \qquad (15)$$

where $g(\phi, \alpha, dm)$ is the gain towards the azimuth angle $\phi$. The PSO algorithm is used to optimize a 10 elements circular dipole array where all array elements are fed at the center and all of them are centered along a circle on the $x$-$y$ plane. The dipoles length is fixed to $\lambda/2$ and the diameters of the dipoles are also fixed to $0.0067\lambda$. The result obtained from PSO algorithm is tabulated in Table 15.

Next, we optimize the same previous array with respect to excitation, separation and dipoles length. The result obtained is tabulated in Table 16. A plot of radiation pattern is shown in Figure 19 compared with the previous result. Results show that slight enhancement is achieved in the maximum SLL and the 3 dB BW by optimizing elements lengths.

## 4. CONCLUSIONS

In this paper, different antenna array types are optimized using the PSO method. This paper illustrates how to model the design of non-uniform antenna arrays for single or multi objective optimization. The well-known method of PSO is proposed as the solution for these design problems. This method efficiently computes the design of several antenna arrays to generate a radiation pattern with desired properties. In the first part of the paper, we dealt with linear arrays. The optimization objectives were: first, minimize the maximum SLL by adjusting the excitation amplitudes, excitation phases or elements positions along the $x$-axis, and then adjust all the previous parameters simultaneously. The numerical results show that the PSO method produces minimum SLL compared with the uniform conventional array and the array obtained from the Tabu search optimization (TSO) method. Second, we minimized the close-in SLL while minimizing the maximum far SLL. Results show that considerable reduction in the close-in SLL is achieved. Third, PSO is used to minimize the average SL power by adjusting all possible array parameters individually and then all of them simultaneously. Results found from PSO show that the average SL power obtained is lower than the uniform conventional array one. Fourth, the array excitation phases are adjusted with PSO to perform beamsteering in certain direction. The PSO is also used to optimize elements locations, excitations amplitude and excitation phases of circular arrays. The results found show that the maximum SLL obtained is lower than the uniform conventional array and GA array, and the array beamwidth is thinner. For practical implementation of circular array, a circular dipole array is optimized to minimize the maximum SLL. The method of moments is used to determine the current distributions on the dipoles. The optimized parameters are elements excitation amplitude, excitation phases, locations and lengths. The results show that minimum SLL can be achieved by optimizing these parameters using the PSO method.

## REFERENCES

1. Schelkunoff, S., "A mathematical theory of linear arrays," *Bell Systems Technology Journal*, Vol. 22, No. 1, 80–107, 1943.
2. Keizer, W. P., "Fast low-sidelobe synthesis for large planar array antennas utilizing successive fast fourier transform of the array factor," *IEEE Trans. on Antennas and Propagat.*, Vol. 55, No. 3, 715–730, March 2007.
3. Woodward, P. M. and J. P. Lawson, "The theoretical precision

with which an arbitrary radiation pattern may be obtained from a source of finite size," *Proc. IEEE*, Vol. 95, No. 1, 120–126, 1948.

4. Dolph, C., "A current distribution for broadside arrays which optimizes the relationship between beamwidth and side-lobe level," Institute of Radio Engineers (IRE), Vol. 34, No. 6, 335–348, 1946.
5. Balanis, C. A., *Antenna Theory Analysis and Design*, 2nd edition, John Wiley & Sons, 1997.
6. Moffett, A. L., "Array factors with non uniform spacing parameters," *IRE Trans. on Antennas and Propagat.*, Vol. 10, 131–136, 1962.
7. Ishimaru, A. and Y. S. Chen, "Thinning and broadbanding antenna arrays by unequal spacings," *IEEE Trans. on Antennas and Propagat.*, Vol. 13, 34–42, 1965.
8. Lo, Y. T. and S. W. Lee, "A study of space tapered arrays," *IEEE Trans. on Antennas and Propagat.*, Vol. 14, No. 1, 22–30, January 1966.
9. Ma, X. and B. K. Chang, "Least square method for optimum thinned antenna arrays," *IEEE Antennas and Propagat. Society International Symposium*, Vol. 4, No. 13, 2232–2235, July 1997.
10. Ng, B. P., "Designing array patterns with optimum inter-element spacings and optimum weights using a computer-aided approach," *Int. J. Electron.*, Vol. 73, No. 3, 653–664, September 1992.
11. Ng, B. P., M. H. Er, and C. A. Kot, "Linear array aperture synthesis with minimum sidelobe level and null control," *IEE Proc. — Microwave Antennas Propagat.*, Vol. 141, No. 3, 2674–2679, June 1994.
12. Ng, B. P., "Array synthesis using a simple computer-aided approach," *Electron. Lett.*, Vol. 26, No. 5, 337–339, March 1990.
13. Ismail, T. H. and M. M. Dawoud, "Null steering in phased arrays by controlling the element positions," *IEEE Trans. on Antennas and Propagat.*, Vol. 39, No. 11, 1561–1566, November 1991.
14. Er, M. H., S. L. Sim, and S. N. Koh, "Application of constrained optimization techniques to array pattern synthesis," *Signal Process*, Vol. 34, No. 3, 323–334, 1993.
15. Steinberg, B. D., "Comparison between the peak sidelobe of random array and algorithmically designed aperiodic arrays," *IEEE Trans. on Antennas and Propagat.*, Vol. 21, 366–369, 1973.
16. Rahmat-samii, Y. and C. G. Christodoulou, "Special issue on synthesis and optimization techniques in electromagnetics and antenna system design," *IEEE Trans. on Antennas and Propagat.*,

Vol. 55, No. 3, 518–522, March 2007.

17. Shavit, R. and I. Taig, "Array pattern synthesis using neural networks with mutual coupling effect," *IEE Proc. Microw. Antennas Propag.*, Vol. 152, No. 5, 354–358, October 2005.
18. Guney, K. and N. A. Sarikaya, "Hybrid method based combining artifical neural network and fuzzy inference system for simultaneous computation of resonant frequencies of rectangular, circular, and triangular microstrip antennas," *IEEE Trans. on Antennas and Propagat.*, Vol. 55, No. 3, 659–668, March 2007.
19. Ng, B. P., "Array synthesis using a simple computer-aided approach," *Electron. Lett.*, Vol. 26, No. 5, 337–339, March 1990.
20. Goldberg, D. E., *Genetic Algorithms in Search, Optimization and Machine Learning*, Addison-Wesley Longman Publishing Co. Inc., Boston, MA, 1989.
21. Tennant, A., M. M. Dawoud, and A. P. Anderson, "Array pattern nulling by element position perturbations using genetic algorithm," *IEEE Electronics Letters*, Vol. 30, No. 3, 174–176, February 1994.
22. Ares, F., S. R. Rengarajan, E. Villanueva, E. Skochinski, and F. Moreno, "Application of genetic algorithms and simulated annealing technique in optimizing the aperture distributions of antenna array patterns," *Electron. Lett.*, Vol. 32, No. 3, 148–149, February 1996.
23. Samii, Y. R. and E. Michielssen, *Electromagnetic Optimization by Genetic Algorithms*, John Wiley and Sons, 1999.
24. Merino, A. R., R. L. Miranda, and J. L. Bonilla, "Optimization method based on genetic algorithms," *Apeiron*, Vol. 12, No. 4, 394–408, October 2005.
25. Marcano, J. D. and F. Duran, "Synthesis of antenna arrays using genetic algorithms," *IEEE Antennas and Propagat. Magazine*, Vol. 42, No. 3, 12–20, June 2000.
26. Haupt, R. L., "Thinned arrays using genetic algorithms," *IEEE Trans. on Antennas and Propagat.*, Vol. 42, No. 7, 993–999, July 1994.
27. Shimizu, M., "Determining the excitation coefficients of an array using genetic algorithms," *IEEE Antennas and Propagat. Society International Symposium*, Vol. 1, No. 20–24, 530–533, June 1994.
28. Yan, K. K. and Y. Lu, "Sidelobe reduction in array-pattern synthesis using genetic algorithm," *IEEE Trans. on Antennas and Propagat.*, Vol. 45, No. 7, 1117–1122, July 1997.
29. Jones, E. A. and W. A. Joines, "Design of Yagi-Uda antennas

using genetic algorithms," *IEEE Trans. on Antennas and Propagat.*, Vol. 45, No. 9, 1386–1392, September 1997.

30. Donelli, M., S. Caorsi, F. Denatala, M. Pastorino, and A. Massa, "Linear antenna synthesis with a hybrid gentic algorithm," *Progress In Electromagnetics Research*, PIER 49, 1–22, 2004.
31. Mohanty, G. K., A. Chakrobarty, and S. Das, "Phase only and amplitude phase synthesis of dual pattern linear antenna arrays using floating point genetic algorithms," *Progress In Electromagnetic Research*, PIER 68, 247–259, 2007.
32. Misra, I. S., R. S. Chakrobarty, and B. B. Mangaraj, "Design, analysis and optimization of V dipole and its three element Yagi-Uda array," *Progress In Electromagnetic Research*, PIER 66, 137–156, 2006.
33. Ferreira, J. A. and F. Ares, "Pattern synthesis of conformal arrays by the simulated annealing technique," *Electron. Lett.*, Vol. 33, No. 14, 1187–1189, July 3, 1997.
34. Kirkpatrick, S., C. D. Gellatt, and M. P. Vecchi, "Optimization by simulated annealing," *Science*, Vol. 220, No. 4598, 671–680, 1983.
35. Murino, V., A. Trucco, and C. S. Regazzoni, "Synthesis of unequally spaced arrays by simulated annealing," *IEEE Trans. on Signal Processing*, Vol. 44, No. 1, 119–123, January 1996.
36. Ares, F., S. R. Rengarajan, E. Villanueva, E. Skochinski, and F. Moreno, "Application of genetic algorithms and simulated annealing technique in optimizing the aperture distributions of antenna array patterns," *Electron. Lett.*, Vol. 32, No. 3, 148–149, February 1996.
37. Rocha-Alicano, C., D. Covarrubias-Rosales, C. Brizuela-Rodriguez, and M. Panduro-Mendoza, "Differential evolution algorithm applied to sidelobe level reduction on a planar array," *AEU International Journal of Electronic and Communications*, Vol. 61, No. 5, 286–290, 2007.
38. Merad, L., F. Bendimerad, and S. Meriah, "Design of linear antenna arrays for side lobe reduction using the tabu search method," *The International Arab Journal of Information Technology*, Vol. 5, No. 3, 219–222, July 2008.
39. Kennedy, J. and R. C. Eberhart, "Particle swarm optimization," *Proc. IEEE Int. Conf. Neural Networks*, Vol. 1942–1948, Piscataway, NJ, 1995.
40. Eberhart, R. C. and Y. Shi, "Particle swarm optimization: Developments, applications and resources," *Proc. Congr. Evolutionary*

*Computation*, Vol. 1, 81–86, 2001.

41. Perez, J. R. and J. Basterrechea, "Comparison of different heuristic optimization methods for nearfield antenna measurements," *IEEE Trans. on Antennas and Propagat.*, Vol. 55, No. 3, 549–555, March 2007.
42. Khodier, M. M. and C. G. Christodoulou, "Linear array geometry synthesis with minimum sidelobe level and null control using particle swarm optimization," *IEEE Trans. on Antennas Propagat.*, Vol. 53, No. 8, 2674–2679, August 2005.
43. Bataineh, M. H. and J. I. Ababneh, "Synthesis of a periodic linear phased antenna array using particle swarm optimization," *Electromagnetics*, Vol. 26, No. 7, 531–541, October 2006.
44. Boeringer, D. W. and D. H. Werner, "Particle swarm optimization versus genetic algorithms for phased array synthesis," *IEEE Trans. on Antennas and Propagat.*, Vol. 52, No. 3, 771–779, March 2004.
45. Nanbo, J. and Y. Rahmat-Samii, "Advances in particle swarm optimization for antenna designs: Real-number, binary, single-objective and multiobjective implementations," *IEEE Trans. on Antennas and Propagat.*, Vol. 55, No. 3, 556–567, March 2007.
46. Dennis, G. and Y. Rahmat-Samii, "Particle swarm optimization for reconfigurable phase differentiated array design," *Microwave and Optical Technology Letters*, Vol. 38, No. 3, 168–175, August 5, 2003.
47. Baskar, S., A. Alphones, P. N. Suganthan, and J. J. Liang, "Design of Yagi-Uda antennas using comprehensive learning particle swarm optimization," *IEE Proc. in Microw. Antennas Propagat.*, Vol. 152, No. 5, 340–346, October 2005.
48. Huang, T. and A. S. Mohan, "A microparticle swarm optimizer for the reconstruction of microwave images," *IEEE Trans. on Antennas and Propagat.*, Vol. 55, No. 3, 568–576, March 2007.
49. Mahmoud, K. R., M. E. El-Adawy, S. M. M. Ibrahem, R. Bansal, and S. H. Zainud-Deen, "Comparison between circular and hexagonal array geometries for smart antenna systems using particle swarm optimization algorithm," *Progress In Electromagnetic Research*, PIER 72, 75–90, 2007.
50. Baskar, S., A. Alphones, P. N. Suganthan, and J. J. Liang, "Design of Yagi-Uda antennas using comprehensive learning particle swarm optimization," *IEEE Microwave Antenna Propagat.*, Vol. 152, No. 5, 340–346, October 2005.
51. Chen, T. B., Y. L. Dong, Y. C. Jiao, and F. S. Zhang, "Synthesis of

circular antenna array using crossed particle swarm optimization algorithm," *Journal of Electromagnetic Waves and Applications*, Vol. 20, No. 13, 1785–1795, 2006.

52. Ciuprina, G., D. Ioan, and I. Munteanu, "Use of intelligent particle swarm optimization in electromagnetics," *IEEE Trans. on Magnetics*, Vol. 38, No. 2, 1037–1040, March 2002.
53. Robinson, J. and Y. Rahmat-Samii, "Particle swarm optimization in electromagnetics," *IEEE Trans. on Antennas and Propagat.*, Vol. 52, No. 2, 397–407, February 2004.
54. Ababneh, J., M. Khodier, and N. Dib, "Synthesis of interdigital capacitors based on particle swarm optimization and artificial neural networks," *International Journal of RF and Microwave Computer-aided Engineering*, Vol. 16, No. 4, 322–330, February 2006.
55. Xu, S. and Y. Rahmat-Samii, "Boundary conditions in particle swarm optimization revisited," *IEEE Trans. on Antennas and Propagat.*, Vol. 55, No. 3, 760–765, March 2007.
56. Alander, J. T., L. A. Zinchenko, and S. N. Sorokin, "Analysis of fitness landscape properties for evolutionary antenna design," *IEEE International Conference on Artificial Intelligent Systems*, 363–368, 2002.
57. Lohn, J. D., W. F. Kraus, D. S. Linden, and S. P. Colornbano, "Evolutionary optimization of Yagi-Uda antennas," *International Conference on Evolvable Systems*, 236–243, Tokyo, October 3–5, 2001.
58. King, R. W. P., "Supergain antennas and the yagi and circular arrays," *IEEE Trans. on Antennas and Propagat.*, Vol. 37, No. 2, 178–186, February 1989.
59. Panduro, M. A., A. L. Mendez, G. Romero, and R. F. Dominguez, "Design of non-uniform circular antenna arrays for side lobe reduction using the method of genetic algorithms," *Vehicular Technology Conference VTC*, Vol. 6, 2696–2700, May 2006.
60. Shihab, M., Y. Najjar, N. Dib, and M. Khodier, "Design of non-uniform circular antenna arrays using particle swarm optimization," *Journal of Electrical Engineering*, Vol. 5, No. 4, 216–220, 2008.
61. Orfanidis, S. J., "Electromagnetic waves and antennas," www.ece.rutgers.edu/orfanidi/ewa., 2003.